The Journal of Neuroscience, February 1993, 13(2): 596–604

Molecular Cloning, Functional Properties, and Distribution of Rat Brain α_7: A Nicotinic Cation Channel Highly Permeable to Calcium

Philippe Séguéla,[1] Jacques Wadiche,[1] Kelly Dineley-Miller,[1] John A. Dani,[1,2] and James W. Patrick[1]

[1]Division of Neuroscience and [2]Department of Molecular Physiology and Biophysics, Baylor College of Medicine, Houston, Texas 77030

A full-length clone coding for the rat α_7 nicotinic receptor subunit was isolated from an adult brain cDNA library and expressed in *Xenopus* oocytes. A significant proportion of the current through α_7-channels is carried by Ca^{2+}. This Ca^{2+} influx then activates a Ca^{2+}-dependent Cl^- conductance, which is blocked by the chloride channel blockers niflumic and fluflenamic acid. Increasing the external NaCl concentration caused the reversal potentials for the α_7-channels and the Ca^{2+}-dependent Cl^- channels to be shifted in opposite directions. Under these conditions, agonist application activates a biphasic current with an initial inward current through α_7-channels followed by a niflumic acid– and fluflenamic acid–blockable outward current through Ca^{2+}-dependent Cl^- channels. A relative measure of the Ca^{2+} permeability was made by measuring the shift in the reversal potential caused by adding 10 mM Ca^{2+} to the external solution. Measurements made in the absence of Cl^-, to avoid artifactual current through Ca^{2+}-activated Cl^- channels, indicate that α_7-homooligomeric channels have a greater relative Ca^{2+} permeability than the other nicotinic ACh receptors. Furthermore, α_7-channels have an even greater relative Ca^{2+} permeability than the NMDA subtype of glutamate receptors. High levels of α_7-transcripts were localized by *in situ* hybridization in the olfactory areas, the hippocampus, the hypothalamus, the amygdala, and the cerebral cortex. These results imply that α_7-containing receptors may play a role in activating calcium-dependent mechanisms in specific neuronal populations of the adult rat limbic system.

[Key words: cholinergic receptor, α-bungarotoxin, ligand-gating, hippocampus, limbic system, calcium]

α-Bungarotoxin (α-BTX) has been extensively used as a quasi-irreversible ligand for the agonist-binding subunit of the nicotinic receptor at the neuromuscular junction (Changeux et al., 1970). α-BTX also binds with high affinity to several central and peripheral neuronal preparations known to contain nicotinic ACh receptors but fails to block nicotinic agonist–mediated responses in these preparations (Patrick and Stallcup, 1977a,b; Vijayaraghavan et al., 1992; see review in Schmidt, 1988). However, the purification of chicken brain α-BTX–binding proteins by affinity chromatography and the N-terminal sequencing of a 48 kDa protein confirmed the homology of this subunit with functional nicotinic receptor subunits (Conti-Tronconi et al., 1985).

Transcripts of genes encoding rat and chick neuronal ACh receptor subunits were discovered by screening various brain and PC12 cDNA libraries with muscle and neuronal subunit probes at low stringency (see review in Deneris et al., 1991). Many of the transcripts thus identified were shown to participate in the formation of nicotinic ACh-gated ion channels when expressed in the *Xenopus* oocyte. The biophysical and pharmacological properties of the receptors formed in the oocyte depend upon which of the various α- and β-subunits contribute to the formation of the receptor (Luetje and Patrick, 1991). The neuronal nicotinic ACh receptors differ from the muscle receptors in two important respects: they are more permeable to calcium ions (Decker and Dani, 1990; Sands and Barish, 1991; Vernino et al., 1992), and they are modulated by calcium ions acting externally (Vernino et al., 1992).

The neuroanatomical distribution of transcripts encoding the α- and β-subunits was revealed by *in situ* hybridization (Wada et al., 1989) and found to correspond qualitatively with the regional pattern of high-affinity ^{3}H-nicotine–binding sites (Clarke et al., 1985), but not with the pattern of high-affinity ^{125}I-α-BTX–binding sites in the rodent brain (Clarke et al., 1985; Härfstrand et al., 1988). This lack of correlation is consistent with the fact that functional rat nicotinic receptors expressed in *Xenopus* oocytes showed no sensitivity to α-BTX (Boulter et al., 1987), strongly suggesting the presence of additional α-BTX–sensitive members of the nicotinic receptor gene family.

Clones encoding avian α_7 and α_8 α-BTX–binding proteins components were isolated by Schoepfer et al. (1990) and Couturier et al. (1990). Chick α_7 was shown to form an α-BTX–sensitive homooligomeric ACh-gated ion channel when expressed in *Xenopus* oocytes. We report here the isolation and functional expression of a clone encoding the rat α_7-subunit and show that the homooligomeric receptor formed with this subunit has an unusually high permeability to calcium ions, an unusual pharmacology, and a specific pattern of expression in the adult rat brain.

Materials and Methods

Molecular cloning of rat α_7. Two degenerate primers, based on conserved and characteristic regions of two chick brain α-BTX–binding protein subunits (Shoepfer et al., 1990) [P1: TGG TT(T,C) CC(A,G,C,T) TT(T,C) GA(T,C) GT(G,A,T,C) CA(A,G) AA(A,G) TG; P2: A(A,G)(A,G) AAC CA(G,A,T,C) GC(A,G) CAC CA(A,G) TT], were synthesized. Rat cDNAs

Received May 27, 1992; revised July 28, 1992; accepted Aug. 3, 1992.

We thank Marietta Piattoni-Kaplan and Gabriele Schuster for expert handling of the oocytes, and William McVaugh for his advice about the reversal potential shift experiments. This project was supported by grants from the NINDS, the NIDA, and the NIH and by a contract from the DOD.

Correspondence should be addressed to Dr. James W. Patrick, Division of Neuroscience, Baylor College of Medicine, One Baylor Plaza, Houston, TX 77030.

(0.5 mg) from whole rat brain, hippocampus, and PC12 cDNA libraries were used as templates for PCR in the presence of 1 mM forward and reverse primers and 2.5 U of Ampli-Taq (Perkin Elmer-Cetus) in 100 μl reactions. Amplification products were analyzed after 45 cycles of the following thermal steps: 1 min of denaturation at 94°C, 1 min of annealing at 52°C, 1 min of extension at 72°C, with slopes of 1°C/sec. Modified versions of the primers including restriction sites for EcoRI in P1 primer and BamHI in P2 primer were used to reamplify the PCR product for subcloning purposes. The expected 582 base pair (bp) fragment was isolated from low-melt agarose, double digested, and subcloned in pBluescript II SK⁻. After sequencing and identification, the random-prime labeled PCR product was used to screen 500,000 plaque-forming units of a whole rat brain size-selected directional cDNA library in λ_{ZAP} [average insert size, 2.4 kilobases (kb); base = 2×10^6] obtained from R. Joho (Frech and Joho, 1989). Duplicate lifts were hybridized at 42°C in 6× saline–sodium citrate (SSC), 50% formamide, 0.5% SDS, 0.1 mg/ml denatured salmon sperm DNA, and then washed under conditions of high stringency at 65°C in 0.1× SSC, 0.5% SDS, without formamide. The complete coding sequence of rat α_7 was deduced by sequencing rescued pBluescript, pLA7-31, from isolated positive clones on both strands by automated sequencing and by the Sanger dideoxy chain termination method with Sequenase (U.S. Biochemicals).

Functional expression in Xenopus *oocytes.* For *in vitro* transcription, the plasmid pLA7-31 containing the complete coding region of the α_7-subunit surrounded by 50 bp of 5′ untranslated region and 1.4 kb of 3′ untranslated region, including an artificial A_{50} tail, was linearized at the 3′ end with NotI, and then transcribed *in vitro* with T7 RNA polymerase in the presence of ^{32}P-UTP. For nuclear injection, the EcoRI α_7-fragment from pLA7-31 was subcloned in the unique EcoRV site of the eukaryotic expression vector pCDNAI/NEO (InVitrogen). Oocytes surgically removed from mature *Xenopus laevis* frogs were treated 2 hr at room temperature with 1 mg/ml type II collagenase (Sigma). The oocytes were defolliculated manually and were microinjected with 10 ng of α_7-cRNA in the cytoplasm or 10 ng cDNA in the nucleus (Ballivet et al., 1990). The α_7 RNA or cDNA was injected alone or coinjected with other nicotinic receptor subunits. For comparisons of voltage–current relationships, the same procedure was applied for expression of other types of nicotinic receptors with 10 ng of α_3- and β_4-cDNA in pcDNAI/NEO (1:1 ratio) and 10 ng of α_1, β_1, γ, and δ in pSM vector (2:1:1:1 ratio). After 2–7 d of expression at 19°C in Barth's solution containing 10 μg/ml gentamycin, oocytes were recorded in a two-electrode voltage-clamp configuration. Oocytes were placed in a 300 ml chamber perfused by gravity (0.5–1 ml/sec) with Ringer's (115 mM NaCl, 2.5 mM KCl, 1.8 mM $CaCl_2$, 10 mM HEPES, pH 7.2) containing 1 mM atropine to block endogenous muscarinic receptors. Drugs were applied by addition to the perfusion solution at room temperature. In reversal potential shift experiments, a chloride-free Ringer's containing 90 mM Na^+ methanesulfonate, 2.5 mM K^+ methanesulfonate, and 10 mM HEPES adjusted at pH 7.2 was used for 24 hr incubation of oocytes (+2 mM Ca^{2+} methanesulfonate) and for recording solution (+1 mM Ca^{2+} or 10 mM Ca^{2+} methanesulfonate). To apply the constant field theory equations (Lewis and Stevens, 1979), the following intracellular concentrations were used: K^+, 92 mM; Na^+, 6 mM; Ca^{2+}, 100 nM. Concentrations, not activities, of ions were used for the calculations. During challenge with nicotinic agonists or antagonists, currents were recorded in real time on an Apple Macintosh II using a Labview II data acquisition virtual instrument (National Instruments) sampling at 1 kHz with a 10 point moving average.

In situ *hybridization in adult rat brain.* The 600 bp PCR fragment in the coding region of α_7 and a 500 bp PvuI fragment in the 3′ untranslated region of plasmid pLA7-31, both subcloned in pBluescript II SK⁻, were used as templates for riboprobe synthesis. After linearization of the plasmids with unique downstream restriction sites, T7 or T3 RNA polymerases were used to transcribe *in vitro* antisense or sense riboprobes in the presence of ^{35}S-UTP. *In situ* hybridization experiments were performed according to Simmons et al. (1989) with minor modifications. Briefly, adult Sprague–Dawley rats (250–300 gm) were deeply anesthetized with an intraperitoneal injection of pentobarbital (0.1 mg/kg), and perfused transcardially first with ice-cold fixative solutions containing 4% paraformaldehyde in 0.1 M sodium acetate buffer (pH 6.5) and then with 4% paraformaldehyde, 0.05% glutaraldehyde in 0.1 M sodium borate buffer (pH 9.5). Blocks of dissected brain were postfixed in 4% paraformaldehyde, 10% sucrose in borate buffer overnight at 4°C. Coronal 25 μm brain sections from the olfactory bulb to the spinal cord were cut frozen on a sliding microtome and mounted on poly-L-lysine–coated slides. Tissue sections were treated with proteinase K (10 μg/ml, 37°C, 30 min), acetylated, dehydrated through graded ethanols, and then vacuum dried. ^{35}S-radiolabeled-RNA probes were applied on mounted sections at a concentration of $5–10 \times 10^6$ cpm/ml at 60°C overnight in an hybridization buffer containing 50% formamide, 0.3 M NaCl, 1 mM Tris (pH 8.0), 1 mM EDTA, 100 μg/ml tRNA, and 1× Denhardt's solution. Sections were rinsed in 4× SSC, digested with RNase A (20 μg/ml, 37°C, 30 min), and finally washed for 30 min under high-stringency conditions, that is, 80°C in 0.1× SSC and 1 mM dithiothreitol, to prevent cross-hybridization of the probe located in the coding region with unknown members of this gene family. To check signal specificity, adjacent sections were incubated with the corresponding sense riboprobe. A light and homogeneous pattern of distribution resulted from these control experiments. Anatomical localization was determined using the stereotaxic atlas of Paxinos and Watson (1986). Sections on slides were then dehydrated in graded ethanols, air dried, and exposed by contact to Betamax films (Amersham) at room temperature for 5–10 d.

Results

Cloning and primary structure of rat α_7-subunit

Sequence analysis of a 2.9-kb-long clone, lZAP-LA7-31, showed a unique 1506 bp open reading frame encoding 502 amino acids (Fig. 1), assuming initiation by the 5′ proximal Met codon, as proposed by Couturier et al. (1990). A polyadenylation signal sequence was found in the 3′ region of the clone. According to the method of von Heijne (1986) and by analogy with N-terminal sequencing data from Conti-Tronconi et al. (1985), we predict that the mature protein is preceded by a typical signal peptide of 22 amino acids that is cleaved between Q_{22} and G_{23}. Three potential sites of N-linked glycosylation (N_{46}, N_{90}, and N_{133}) in the N-terminal extracellular domain of the protein are conserved between the rat and the chicken homologs. The cysteine loop conserved in most ligand-gated ion channels (Galzi et al., 1991) is present in α_7, as well as the pair of adjacent cysteine residues characteristic of both muscle and neuronal agonist-binding subunits. An extracellular cysteine residue in position aa_{138} is also conserved between chick and rat α-BTX–binding protein subunits. In addition to the leader sequence, four putative α-helix transmembrane domains corresponding to four stretches of 19–24 amino acids (TMD I–IV) showed a significantly higher hydropathy index according to Kyte–Doolitle algorithm (Kyte and Doolitle, 1982). Multiple putative phosphorylation sites were identified in the large cytoplasmic domain of the protein deduced to lie between TMD III and TMD IV. Consensus sites exist for the phosphorylation of S_{365} by cAMP-dependant protein kinase, of T_{415} and S_{427} by casein kinase II, and of Y_{442} by tyrosine kinase (Kemp and Pearson, 1990) (Fig. 1). No site for protein kinase C was found in the predicted intracellular domains of the protein. The homology of rat α_7 with other rat nicotinic receptor subunits, in the extracellular domain (aa_1–aa_{204}) containing the agonist-binding site, was found to be 38% with α_1, 43% with α_3, 39% with α_5, and 40% with β_2 at the amino acid level. Thus, the weak homology of rat α_7 with other nicotinic subunits places this protein, with chick α_7 and α_8, in a subgroup of phylogenetically related but nevertheless distant members of the ACh-gated cation channel gene family.

Functional expression in Xenopus *oocytes*

α_7-Subunits expressed in oocytes after RNA or cDNA injection form functional cation channels gated by nicotinic agonists. This homooligomeric ACh-gated channel desensitizes more rapidly than other nicotinic receptors (Revah et al., 1991) and recovers completely in a short period of time in the presence of nonde-

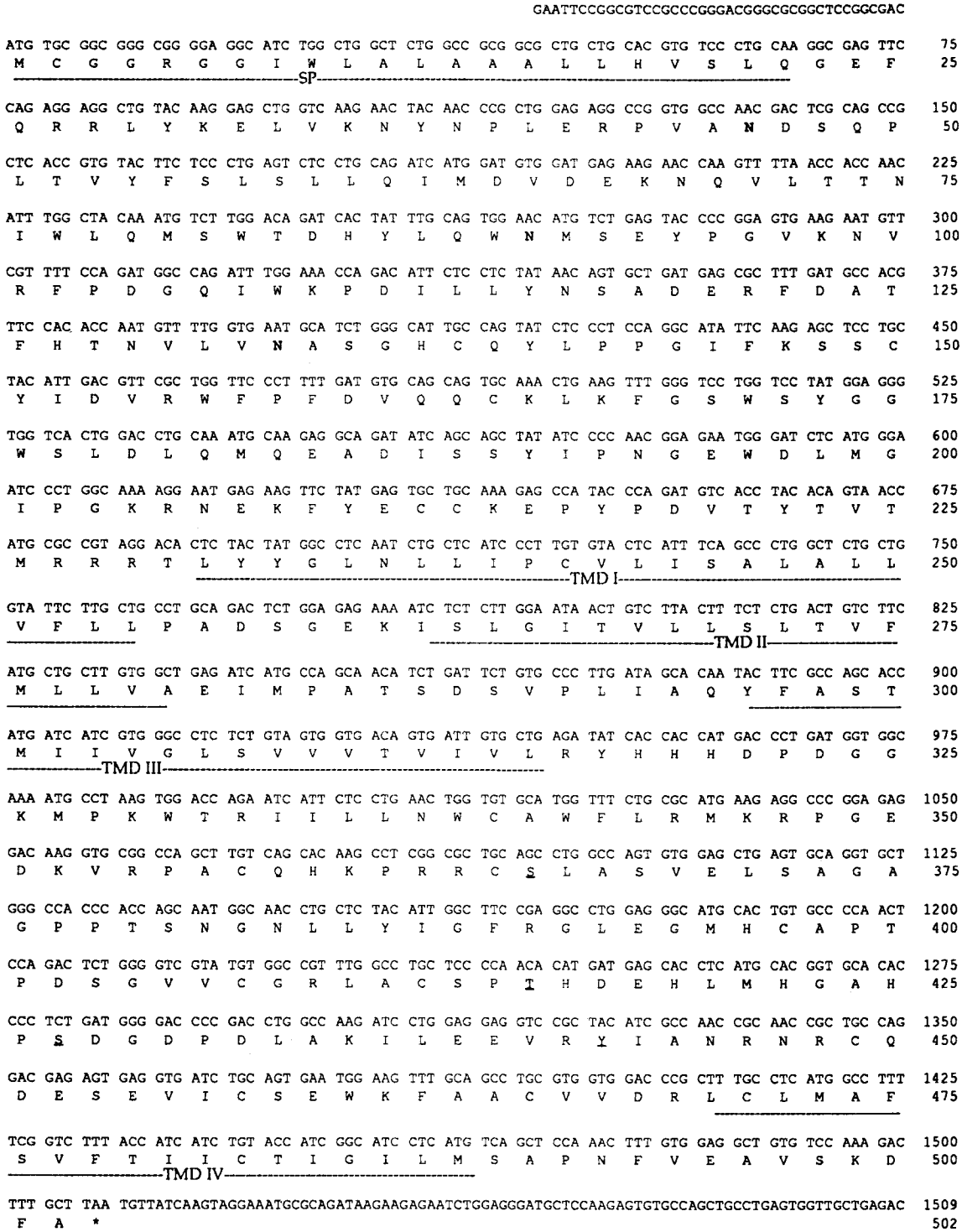


```
TTGCTGATCCTGGTTGCATGAAGATTCAGCTTTCGTGGTTCGGGTCCCTGGAGTCATTCCTCTGCCCTGAGAGGAAGATGAAAGATTCTTCTTCATCCT
TTGTCATCACAGAGATTTTGCCGTTGCTGCAGTCAGTGTTACCGCTGCGTGTGTCCCGTCCCACTATGGCCCGCTCTCTGACCCTCTGTGCACTGCTGC
TTGCTGGAGAAGACTGGACTCCAGCCGTTGCTGCCCCCTTCATTCCCTGGTGACTCTTGCTGCCTTAACTGGTCATTTTACAGACTGTAGCTTCACAGG
AATGCCACCTGCGTAAAGCTGCTGTGGACTGGGGAATTCTGCCCTGGTTGTACAGATCTCAGAAATGGTTCCATTGTCTGCTGGTTGTTCCAGAGAAAA
ATGACTGATCCTGAACTGTCCTGGACTTGACACTTTCGCTGCTATTGTAGCAGCCATTACTGCTGCAGACATTGTGTCTGCAGTGTCTGGAGTTATCCT
CCCCCAATCTATTGTTAGACAAACACAGTGGGTAAACTTTCTGGAGTAGTTACTAACAATTGGGAATTCTAAATTCTATTATAGGAGCGGCTTGACTAC
GGCCCTTGGTGGTAACAGCTGAGGTGAACCAGATGAGGTGCCCGCTATTTATCGGGAGTGGCTCTGTTTGGTGCAGCCCTATGCTGTGGATTAGTGTTC
ATGCTGTGGTTGGTTTGCAAACTCAGATCTCAACAGAAACGTGACAAGGCCGTTATCACTCAAGCACTTGTGGTCATTGTACAAGGGGCCTCCCCTGGA
ATTTGGTTATCTATGCTCAGGAATTAGTTGGTATCTGAGTTCTCTGCTCTTGCACCCCATGGATCTGTGGATCCATTGCACTGGGATGAGAGAGACTCA
ATGATCCTTTGATCAGCCCTTCCACATCGCTGAGGTTTCCTCATTGCACGCGATAGGGTGATCATGATTTGTTATAAAATAAATGATTTGTGATAAATT
ATAAATAAATAGGGGGAGATGTAGAGGGCCGCTTTAACATTCGCCACCACAAGATGGCGCTGGCTTCCACTGTGCCCCACGGGGAAGGCCAGGATAGCT
TCTGCCATTACAAGATGGCGCTGGCCTCCGCCGCCGAGCCGACTTCCTTTCAGGAAGTTAACTGTGTGCGCATGTGCAAGAGTGCCTTCGTGCCAGGTC
TTTGCCCACTCTGGGGCGTGCCTAATGAGATCATGGGTAAGCGACCAATCAGGTGTGGATGTGCCGCACTAGGGTGTATATGAGCCGCGCCATGCAGGC
GCGCGGGGCTCTCTTTAAGATTTAATAAAAGTTTTGGCTGCTGTAAGGAAAAAAAAAAAAAAAAAAAAAAAAAAAAAAAAAAAAAAAAAAAAAAAAA
AAAGCCG
```

Figure 1. Nucleotide and deduced sequences of the clone λ_{ZAP}-LA7-31 encoding rat α_7-subunit. Numbering of amino acids begins with the first Met codon of the longest open reading frame. Predicted membrane spanning domains (*TMD I–IV*) and signal peptide (*SP*) are *underlined.* Postulated *N*-glycosylated asparagine residues are indicated in *boldface.* Residues found in consensus sites of phosphorylation in the large intracellular domain of the protein between *TMD III* and *TMD IV* are *underlined.*

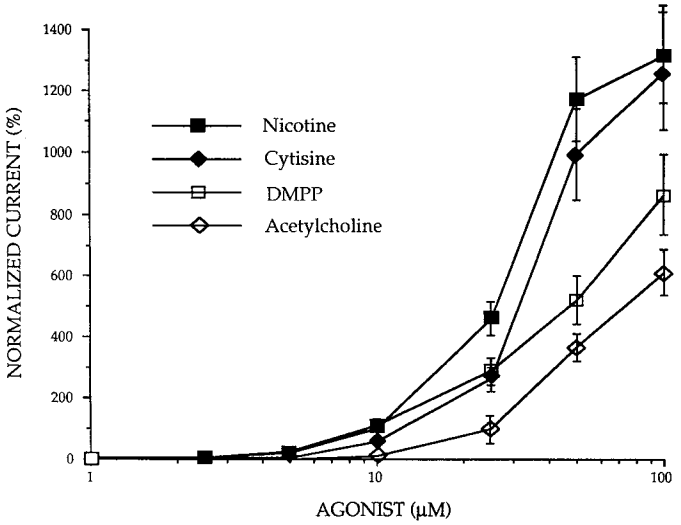

Figure 2. Profile of sensitivity of homooligomeric rat α_7-receptors to nicotinic agonists. Agonist-induced current responses of oocytes expressing rat α_7-receptors were recorded under two-electrode voltage clamp at a holding potential of −60 mV. Currents were elicited by application of 1–100 μM nicotine (*solid squares*), cytisine (*solid diamonds*), DMPP (*open squares*), and ACh (*open diamonds*). Peak currents are represented after normalization to the response of the oocyte to 10 μM nicotine (100%). Each point corresponds to the mean ± SD of the responses of three to five different oocytes.

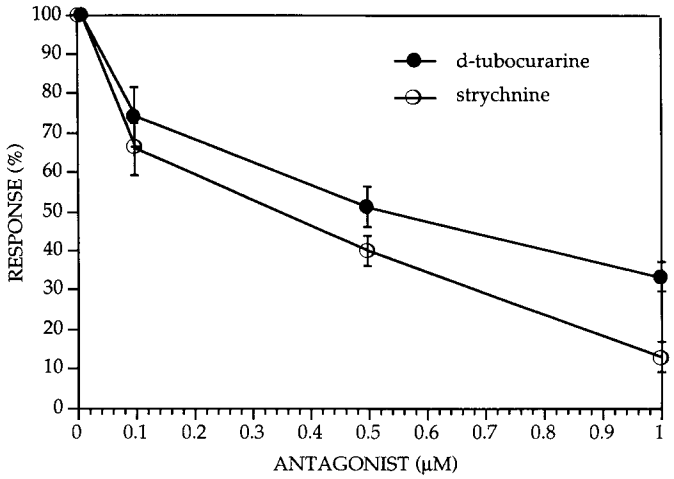

Figure 3. The alkaloids strychnine and *d*-tubocurarine are antagonists of rat α_7-receptors. At a holding potential of −60 mV, peak currents were recorded from oocytes expressing α_7-receptors during challenge with 20 μM nicotine coapplied with various concentrations of strychnine and *d*-tubocurarine. The reduction in current (blockade) was plotted in percentage of control versus the antagonist concentration. IC_{50} values were determined to be 0.35 mM for strychnine and 0.55 μM for *d*-tubocurarine. Each point corresponds to the mean ± SD of the responses of three different oocytes.

sensitizing concentrations of agonists. The α_7-receptor is moderately sensitive to ACh and displays the following order of potency: nicotine > cytisine > DMPP > ACh (Fig. 2). Atypically, DMPP was found to be more potent than cytisine when applied below the 10 μM concentration range but less potent at higher concentrations. It is possible that this result is a consequence of some channel-blocking activity (Sine and Steinbach, 1984) (Fig. 2) or a consequence of missing the earliest peak of the current because of desensitization and the relatively slow solution changes with the oocytes.

α_7-Receptors expressed in the oocyte were found to be highly sensitive to α-BTX and were completely blocked by nanomolar concentrations of the neurotoxin. The alkaloid strychnine, classically used as a blocker of central glycine-gated chloride channels, was found to block activation of α_7-homooligomers with an IC_{50} of 0.35 μM, which is approximately the same potency as the antagonist *d*-tubocurarine (IC*50* of 0.55 μM) in this expression system (Fig. 3).

The α_7-gene is expressed in PC12 cells. Pairwise coexpression in oocytes of α_7 with other nicotinic receptor subunits (α_3, α_5, β_2, β_4) that are known to also be expressed in PC12 cells did not lead to the formation of receptors pharmacologically distinct from α_7 alone, suggesting that α_7 did not associate with these subunits under these experimental conditions. It is unlikely that a heterooligomer with the same pharmacology as the α_7-homooligomer was formed because the current recorded after coinjection of α_7 and other nicotinic subunits was proportional only to the amount of α_7 RNA or cDNA injected and was not proportional to the total amount of message injected (data not shown).

Ca^{2+} permeability of α_7-channels

As illustrated in Figure 4, the nicotine-induced current recorded from homooligomeric α_7-channels was dramatically reduced after addition of the chloride channel blockers niflumic acid, and fluflenamic acid (White and Aylwin, 1990). On average, the total current was reduced by 80% at a holding potential of −60 mV in the presence of 100 μM niflumic acid and fluflenamic acid in normal Ringer's. This blockade might have resulted from a direct antagonist action of these compounds on the α_7-receptor (Lerma and Del Rio, 1992). Alternatively, it might have resulted from blockade of endogenous Ca^{2+} activated chloride channels present in the membrane of *Xenopus* oocytes (Miledi and Parker, 1984; Vernino et al., 1992) that were opened by the Ca^{2+} flowing through the nicotine-activated α_7-channels. Because the reversal potential of chloride current in the oocyte is about −25 mV, currents through both the α_7-channel and the Cl^- channel would appear as inward cationic current at potentials below −25 mV and the current through these two channel types would add at the holding potential of −60 mV used in Figure 4.

To separate activation of α_7-channels from the subsequent activation of the Ca^{2+}-dependent Cl^- channels, we shifted the reversal potentials of chloride and sodium in opposite directions by transiently increasing the external NaCl concentration to 350 mM. Then, agonist application produced an inward current through α_7-channels and a distinguishable outward current through the Ca^{2+}-dependent chloride channels. The consequence of activating the α_7-receptor under these conditions is illustrated in Figure 5*A*, where the initial inward current (labeled 1) is quickly followed by a larger outward current (labeled 2). Application of the chloride channel blockers does not block the initial inward current (labeled 1 in Fig. 5*B*), but abolishes most of the subsequent outward current (labeled 2). This result shows that the reduction in α_7-current under normal conditions is not simply a result of a direct blockade of α_7-receptors but rather is due to blockade of the secondary Ca^{2+}-dependent chloride current. Because α_7-channels activate the Ca^{2+}-dependent Cl^- channels better than other types of nicotinic receptors, the α_7-receptor seems to be more permeable to Ca^{2+} than are muscle and other neuronal nicotinic receptors (Decker and Dani, 1990; Vernino et al., 1992).

We examined the relative Ca^{2+} permeability of the α_7-receptor by measuring changes in the reversal potential of the nicotine-

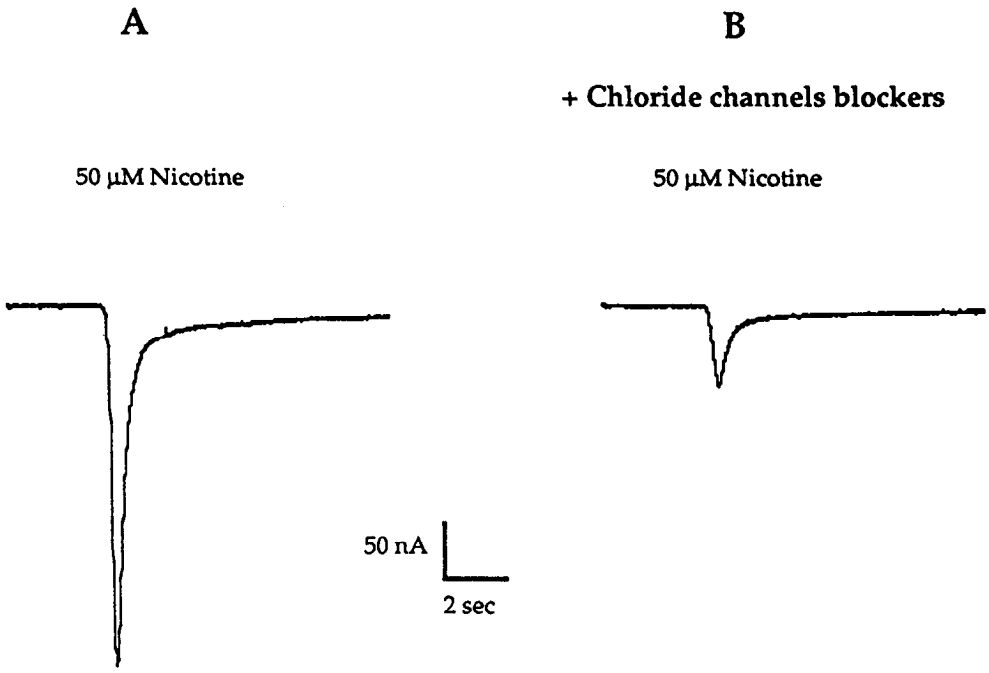

Figure 4. Nicotine-induced current in the absence or presence of Ca^{2+}-activated chloride channel blockers. Currents induced by 50 μM nicotine at a holding potential of −60 mV are shown from a single oocyte expressing α_7-channels bathed in our normal Ringer's solution. Agonists with or without blockers were delivered into the chamber, and, owing to mixing in the chamber, a low concentration of agonist was present for a short time after washout began. Therefore, there is a small current after washout that is seen during the short (12 sec) current traces. *A*, This current was induced before the oocyte was exposed to niflumic acid and fluflenamic acid, which are blockers of the Ca^{2+}-activated Cl^- channels. *B*, After a 20 min bath preincubation with the blockers and then coapplication of the nicotine with 100 μM niflumic acid and fluflenamic acid, there is a large reduction in the current. The results indicate that Ca^{2+} influx through α_7-channels is inhibited, at least partially, in *B* by the blockers. If the blockers are completely washed out, the current recovers to nearly the same amplitude seen in *A*.

induced current while changing the external Ca^{2+} concentration from 1 mM to 10 mM. To prevent contamination of the measurement by activation of the endogenous Ca^{2+}-activated chloride channels, we first measured the reversal potential shift in the presence of chloride channel blockers. Even at high concentrations of niflumic and fluflenamic acid (150 μM each), we were unable to prevent always and completely the activation of the chloride current in 10 mM external Ca^{2+} (data not shown). Consequently, we removed chloride ions from the recording solution and from the oocytes by incubating them 24 hr or more in chloride-free methanesulfonate-based Ringer's. Only under these conditions were we able always to avoid a significant activation of Ca^{2+}-dependent chloride current.

The reversal potentials of the mouse muscle nicotinic receptor ($\alpha_1\beta_1\gamma\delta$-type), the rat $\alpha_3\beta_4$-neuronal receptor, and the rat α_7 receptor were measured in 1 mM and 10 mM Ca^{2+} in chloride-free methanesulfonate-containing Ringer's. We measured reversal potential shifts of +3 ± 2 mV for the muscle receptor, +7 ± 2 mV for the neuronal $\alpha_3\beta_4$-receptor, and 29 ± 3 mV for the α_7-receptor (Fig. 6). Additional care was taken to be certain the large shift in the α_7 reversal potential was not influenced by the Ca^{2+}-dependent Cl^- conductance. The reversal potential shift observed was found to be insensitive either to the chloride channel blockers niflumic acid and fluflenamic acid (50 μM each) in the Cl^--free bathing solution, or to the replacement of 3 M KCl with 4 M cesium methanesulfonate and 50 mM CsCl

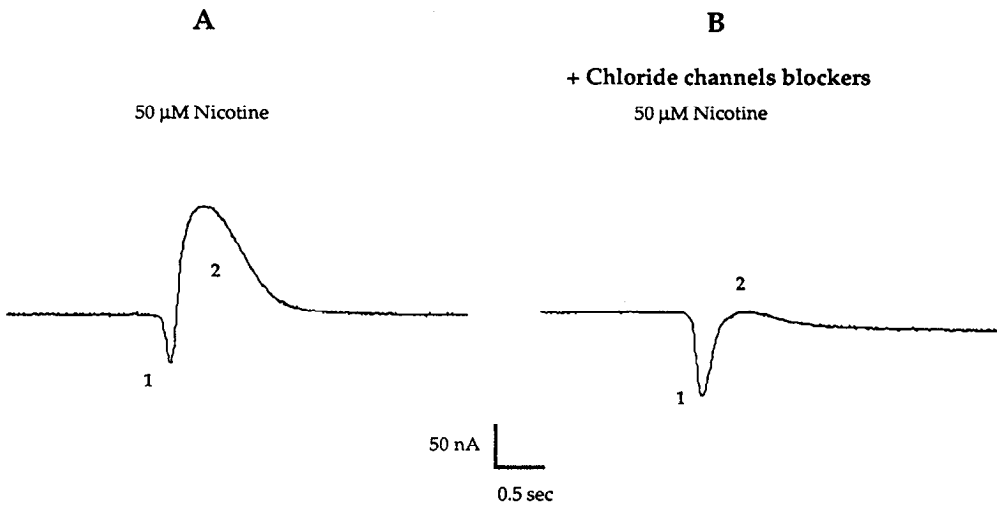

Figure 5. Nicotine-induced currents show two components when the Na^+ and Cl^- reversal potentials are separated. *A*, After transient increase in external NaCl (350 mM), 50 μM nicotine induced a small inward current (*1*) followed by a major outward current (*2*), at a holding potential of −23 mV. Under these conditions, the inward current through the α_7-channels subsequently activates the outward current through the Ca^{2+} activated Cl^- channels. *B*, At the same holding potential, after 20 min preincubation of the oocyte in 100 μM niflumic acid and fluflenamic acid, 50 μM nicotine elicited a predominately inward cationic current (*1*) while the outward chloride component (*2*) is greatly reduced. The visualization of these two components indicates that in normal Ringer's and at potentials below the reversal potential of chloride current, most of the observed nicotine-induced current is due to the secondary activation of Ca^{2+}-activated chloride channels.

in the voltage-clamp recording electrodes. Since the relative permeability of these cation-selective channels to Ca^{2+} versus Na^+ is a function of the magnitude of the shift of the reversal potential, these results indicate that the relative permeability of the α_7-receptor to Ca^{2+} is greater than that of the other nicotinic receptors (Sands and Barish, 1991; Vernino et al., 1992) and of the NMDA subtype of glutamate receptors (Mayer and Westbrook, 1987; Iino et al., 1990). According to the constant field theory, the shift of reversal potential of +29 mV observed for α_7-induced current would correspond to a permeability ratio (P_{Ca}:P_{Na}) of about 20 (see Materials and Methods).

Anatomical distribution of α_7-transcripts

Transcripts encoding the α_7-subunit were found in discrete neuronal populations throughout the adult rat brain. An overview of the distribution of α_7-transcripts in coronal sections of adult rat CNS is presented in Figure 7. This α-BTX–binding subunit is highly expressed in olfactory regions, mainly in the accessory olfactory bulb, tania tecta, and anterior olfactory nucleus (Fig. 7*A–D*). High transcription levels are also observed in the primary olfactory cortex, in the endopiriform nucleus, and in the claustrum. Moderate to high hybridization signal was localized in superficial and deep layers of the isocortex from the frontal to the occipital areas. Intense hybridization was detected in the hippocampal formation, where most of the staining corresponded to the granule cell layer in the dentate gyrus and the pyramidal cell layers in fields CA4, CA3, CA2, and CA1. Nevertheless, intensely labeled interneurons were identified in the stratum oriens and stratum moleculare of fields CA4–CA1. As illustrated in Figure 7*D*, a significant difference in the degree of hybridization occurs in the pyramidal cell layer at the boundary between fields CA3 and CA1. The same boundary is observed in the input of mossy fibers terminals and in the transcription level of the β_2-subunit (Wada et al., 1989) and may simply reflect the change from a multiple pyramidal cell layer in field CA3 to a single pyramidal cell layer in field CA1. Weak to moderate signals were observed in the subiculum and entorhinal cortex. A strong hybridization signal for the α_7-subunit was found in the amygdala, mainly in posteromedial cortical amygdaloid nucleus and amygdalohippocampal area. Most of the nuclei in periventricular, medial, and lateral zones of the hypothalamus contained α_7-mRNA, including the suprachiasmatic, arcuate, supraoptic, dorso- and ventromedial nuclei, the mammillary complex, and the medial preoptic area. Zona incerta, LGN, subthalamic nucleus, medial habenula, and interpeduncular nuclei have also detectable levels of α_7-transcripts. Moderate to strong hybridization was observed in superior and inferior colliculi, respectively. In the brainstem, α_7-subunits are expressed in the central gray, in the dorsal and median raphe nuclei, in the tegmental nuclei, and in the dorsal and ventral nuclei of the lateral lemniscus. In cerebellum, weak hybridization was observed only in the Purkinje cell layer (Fig. 7*E*). A high level of transcription was detected in the vestibular nuclei. In the spinal cord, a moderate α_7-signal was localized throughout substantia gelatinosa, central gray, and ventral horn (Fig. 7*F*).

Discussion

Functional properties of α_7-homooligomers

Rat α_7 is clearly a member of the nicotinic ACh receptor gene family. The encoded protein has the general architectural features of the proteins encoded by this gene family and has the two extracellular adjacent cysteine residues characteristic of agonist-binding subunits (Galzi et al., 1991). It differs from the other members of the family in that it has an additional cysteine residue in the extracellular domain and it forms functional receptors in the absence of other subunits. In the case of the chicken α_7-gene, the intron–exon structure further distinguishes the α_7-gene from the other members of the gene family (Couturier et al., 1990).

The α_7-homooligomeric receptor differs pharmacologically from other nicotinic receptors. The α_7-receptor is blocked by α-BTX. This property is only shared by the muscle receptor in the rat nicotinic receptor family. In addition, the α_7-receptor is inhibited by strychnine, which is a high-affinity antagonist of central glycine-gated Cl^- channels (Grenningloh et al., 1987). Affinities of strychnine for α-BTX–binding sites in the micromolar range have been previously reported in preparations of *Aplysia* ganglia and rat brain membranes (Ono and Salvaterra, 1981). However, the most important characteristic of the α_7-cation channel remains its marked permeability to Ca^{2+} ions.

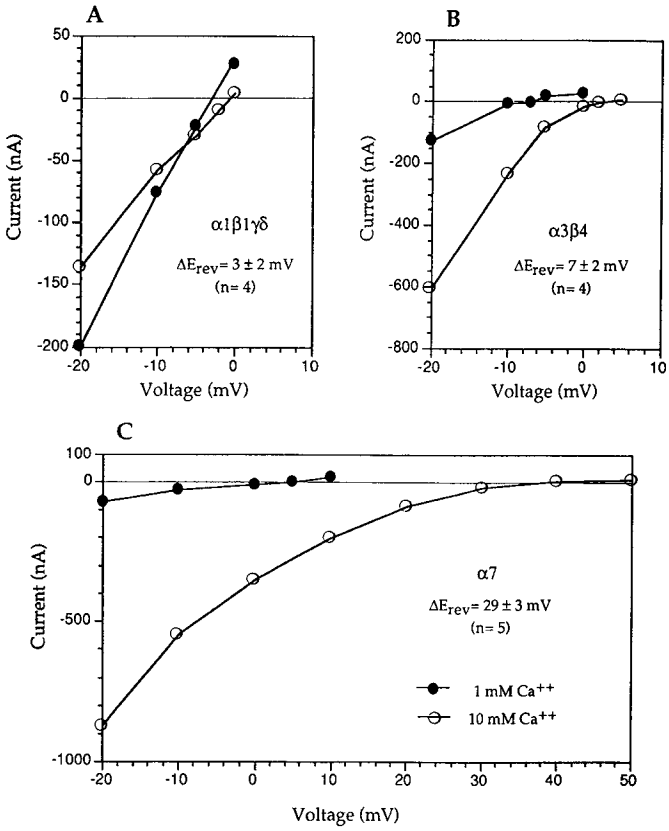

Figure 6. Reversal potential shift comparisons between muscle (*A*), $\alpha_3\beta_4$ (*B*), and α_7 (*C*) cation channels expressed in *Xenopus* oocytes. Peak currents elicited by 2 μM ACh ($\alpha_1\beta_1\gamma\delta$), or 20 μM nicotine ($\alpha_3\beta_4$ and α_7) were measured at different holding potentials and plotted as a function of membrane potential (voltage) in chloride-free Ringer's containing 1 mM Ca^{2+} (*solid circles*) and 10 mM Ca^{2+} (*open circles*). To remove internal Cl^-, the oocytes were preincubated 24 hr in chloride- and magnesium-free methanesulfonate-based recording buffer before measurements. Reversal potential shift values (ΔE_{rev}) correspond to the mean ± SD of the number (n) of measurements made in different oocytes. The current–voltage relationships illustrated are representative of the experiments performed for each combination of nicotinic receptor subunits. As expected from previous work, external Ca^{2+} decreases the amplitude of the response of muscle nicotinic ACh receptors (see Decker and Dani, 1990) but increases the response of neuronal nicotinic ACh receptors (see Vernino et al., 1992) and of α_7-receptors.

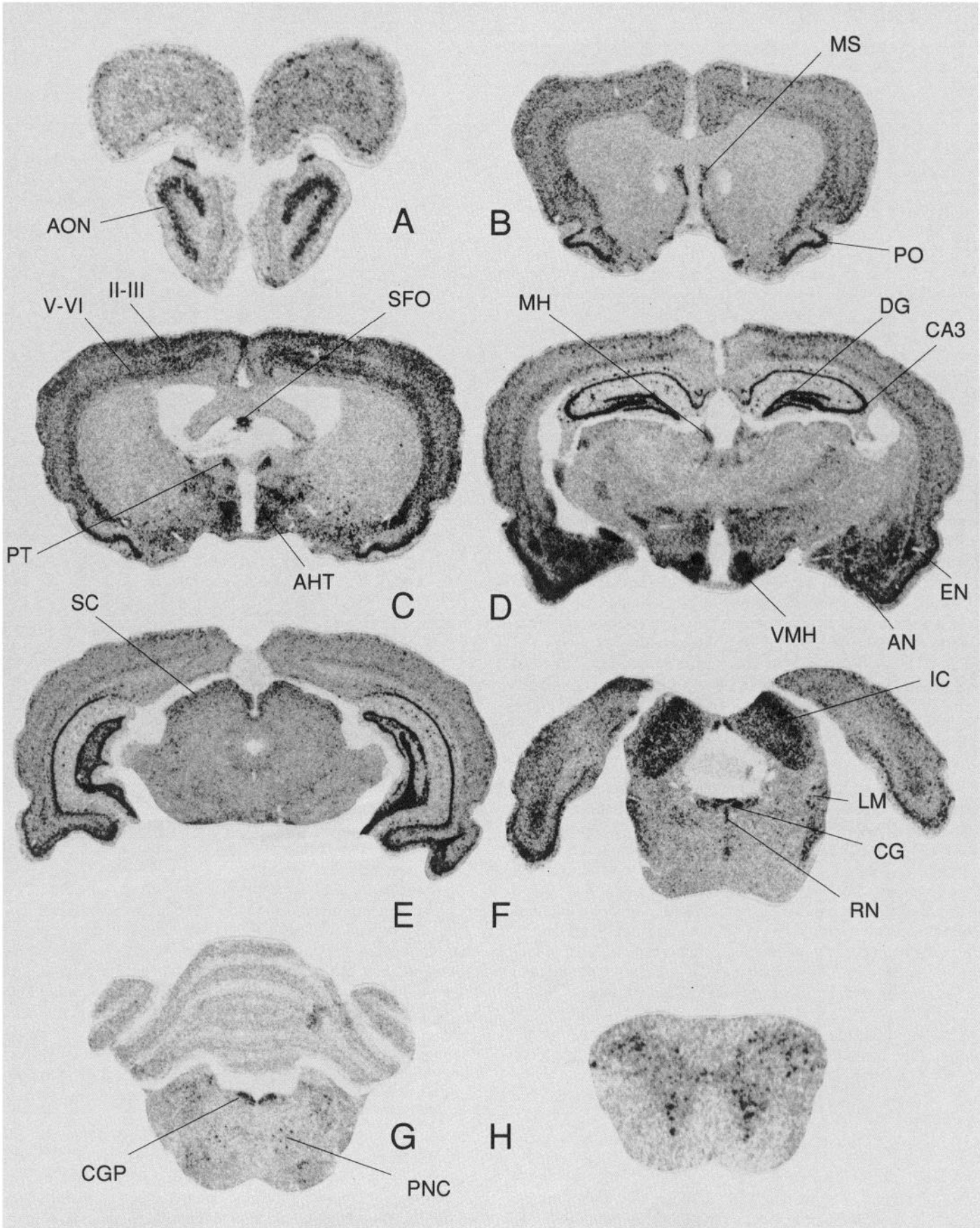
AON
A
MS
B
PO
V-VI
II-III
SFO
PT
AHT
C
MH
DG
CA3
EN
VMH
AN
D
SC
E
IC
LM
CG
RN
F
CGP
PNC
G
H

We have demonstrated here that the major portion of the current observed upon activation of this receptor in the oocyte results from secondary activation of endogenous Ca^{2+}-dependent Cl^- channels and that the characteristics of this Cl^- current dominate the apparent nicotinic α_7-response. We have separated the α_7-response from the Cl^- channel response by using specific blockers of this chloride current. Furthermore, we have demonstrated an α_7-current under conditions in which there is minimal contribution from Cl^- channels and have shown that Ca^{2+} ions play a major role in determining the reversal potential of cation-selective α_7-channels.

We have tried to place the apparent relative Ca^{2+} permeability of the α_7-homooligomer within the context of the permeabilities of other known ligand-gated ion channels. A Ca:Na permeability ratio (P_{Ca}:P_{Na}) of 0.2 was reported for the muscle nicotinic receptor (Adams et al., 1980; Vernino et al., 1992) and P_{Ca}:P_{Na} is about 1.5 for the neuronal nicotinic receptors present in chromaffin cells (Vernino et al., 1992) or in PC12 cells (Sands and Barish, 1990). We can infer from the shift of reversal potential observed in our experimental conditions that the P_{Ca}:P_{Na} ratio for the rat α_7-channel is around 20, higher than the P_{Ca}:P_{Na} ratio of 5 reported for the NMDA subtype of glutamate receptors (Mayer and Westbrook, 1987; Iino et al., 1988). Application of nicotine to chick ciliary ganglion neurons results in an α-BTX–sensitive increase in cytoplasmic calcium (Vijayaraghavan et al., 1992). Our data suggest that at least a portion of this increase could result from the calcium flux through an α_7-type receptor.

α_7 is a major component of α-BTX–binding proteins in the rat brain

As illustrated in Figure 7, the distribution of α_7-transcripts in the adult rat brain does not correlate with the distribution of high-affinity ^{3}H-nicotine–binding sites in the rat brain but overlaps the pattern of ^{125}I-α-BTX–binding sites observed by ligand-binding autoradiography (Clarke et al., 1985). This, plus the observation that α-BTX blocks activation of the α_7-receptor in the oocyte suggests that α_7 is a component of rat brain α-BTX–binding proteins.

Despite the marked difference with the distribution of high-affinity nicotine-binding sites, the distribution of α_7-mRNA in the rat brain remains compatible with the immunohistochemically defined cholinergic pathways (for review, see Wainer and Mesulam, 1990). Interestingly, most of the structures with the highest abundance of α_7-transcripts and high-affinity α-BTX in binding sites, that is, the olfactory regions, the hippocampus, the amygdala, and the hypothalamus, are main components of the limbic system and thus correspond to functionally related neuronal populations. It is also noteworthy that strains of mice with high sensitivity to nicotine-induced seizures displayed higher densities of α-BTX–binding sites in the hippocampus (Miner et al., 1986) and that α-BTX and nicotine have been shown to compete for a population of low-affinity nicotine-binding sites in the rat brain (Wonnacott, 1986).

Composition of native α-BTX–binding proteins

α_7 is not consistently coexpressed with other known agonist-binding subunits, suggesting that association of α_7 with other subunits in functional receptor subtypes is not the general rule in the adult brain. The most likely alternatives are that α_7-subunits form homooligomers *in vivo* or that α_7-subunits are combined with unknown subunits in uncharacterized receptor subtypes. Vertebrate α-BTX–binding proteins have been affinity purified from chick optic lobe (Conti-Tronconi et al., 1985), mouse (Seto et al., 1981), or rat brain (Kemp et al., 1985; Whiting and Lindstrom, 1987), and from PC12 cells (Kemp et al., 1988) and IMR32 cells (Gotti et al., 1990). These purifications generated preparations containing multiple components ranging in size from 46 kDa to 72 kDa. These results are consistent with the existence of heterooligomeric α-BTX–binding proteins. The calculated molecular weight of the nonglycosylated, mature α_7 is 54,200 Da. We suggest that the α_7-subunit corresponds to the major 55–60 kDa protein in α-BTX–binding protein preparations. This protein contains a binding site for α-BTX and is labeled by the alkylating agent MBTA. Experiments using subunit-specific antisense oligonucleotides (Listerud et al., 1991) suggest that heterooligomeric receptors containing both α_7- and α_3-subunits are found in chick ciliary ganglion neurons. In view of the pharmacology of α_7-receptors and their membership in the nicotinic receptor gene family, the absence of an α-BTX–sensitive nicotine-induced current in PC12 cells and in other neuronal preparations known to express this subunit (see review in Schmidt, 1988) suggests either that the blockade by α-BTX is sensitive to heterooligomeric association or that the experimental conditions used to detect the activation of α_7-containing receptors are inadequate. In any case, the high Ca^{2+} permeability of the α_7-channel may confer to the nicotinic receptors containing this subunit the ability to increase intracellular Ca^{2+} and thus to trigger Ca^{2+}-dependent cytoplasmic events in cholinoceptive neurons, even in conditions where the voltage-gated Ca^{2+} channels are not operational. This hypothesis would be consistent with the reports of a marked developmental regulation of α_7 at the transcription level (Couturier et al., 1990) correlated with an increase in the density of α-BTX–binding sites (Fiedler et al., 1987; Fuchs, 1989) during critical stages of synaptogenesis in the vertebrate brain.

References

Adams DJ, Dwyer TM, Hille B (1980) The permeability of endplate channels to monovalent and divalent metal cations. J Gen Physiol 75:49–510.

Ballivet M, Nef P, Couturier S, Rungger D, Bader CR, Bertrand D, Cooper E (1990) Electrophysiology of a chick neuronal nicotinic acetylcholine receptor expressed in *Xenopus* oocytes after cDNA injection. Neuron 1:847–852.

Boulter J, Connolly J, Deneris E, Goldman D, Heinemann S, Patrick J (1987) Functional expression of two neuronal nicotinic acetylcholine receptors from cDNA clones identifies a gene family. Proc Natl Acad Sci USA 84:7763–7767.

←

Figure 7. Distribution of α_7-mRNA in the adult rat brain. Representative 25-μm-thick coronal sections from adult rat brain were hybridized *in situ* at high stringency with ^{35}S-UTP–labeled rat α_7-riboprobes (see Materials and Methods). *II-III*, isocortex, layers II–III; *V–VI*, isocortex, layers V–VI; *AHT*, anterior hypothalamus; *AN*, amygdaloid nuclei; *AON*, anterior olfactory nucleus; *CA3*, field CA3 of Ammon's horn; *CG*, central gray; *CGP*, central gray pons; *DG*, dentate gyrus; *EN*, endopiriform nucleus; *IC*, inferior colliculus; *LM*, lateral lemniscus nuclei; *MH*, medial habenula; *MS*, medial and lateral septum; *PNC*, pontine reticular nucleus; *PO*, primary olfactory cortex; *PT*, parathenial thalamic nucleus; *RN*, raphe nuclei; *SC*, superior colliculus; *SFO*, subfornical organ; *VMH*, ventromedial hypothalamus. Magnification: *A*, 9×; *B–D*, 7×; *E–G*, 6×; *H*, 11×.

Changeux J-P, Kasai M, Lee CY (1970) The use of a snake venom toxin to characterize the cholinergic receptor protein. Proc Natl Acad Sci USA 67:1241–1247.

Clarke PBS, Schwartz RD, Paul SM, Pert CB, Pert A (1985) Nicotinic binding in rat brain: autoradiographic comparison of [^{3}H] acetylcholine, [^{3}H] nicotine, and [^{125}I]-α-bungarotoxin. J Neurosci 5:1307–1315.

Conti-Tronconi BA, Dunn SMJ, Barnard EA, Dolly OJ, Lai FA, Ray N, Raftery MA (1985) Brain and muscle nicotinic acetylcholine receptors are different but homologous proteins. Proc Natl Acad Sci USA 82:5208–5212.

Couturier S, Bertrand D, Matter J-M, Hernandez M-C, Bertrand S, Millar N, Valera S, Barkas T, Ballivet M (1990) A neuronal nicotinic acetylcholine receptor subunit (α7) is developmentally regulated and forms a homo-oligomeric channel blocked by α-BTX. Neuron 5:847–856.

Decker ER, Dani JA (1990) Calcium permeability of the nicotinic acetylcholine receptor: the single-channel calcium influx is significant. J Neurosci 10:3413–3420.

Deneris ES, Connolly J, Rogers SW, Duvoisin R (1991) Pharmacological and functional diversity of neuronal nicotinic acetylcholine receptors. Trends Pharmacol Sci 12:34–40.

Fiedler EP, Marks MJ, Collins AC (1987) Postnatal development of cholinergic enzymes and receptors in mouse brain. J Neurochem 49: 983–990.

Frech GC, Joho RH (1989) Construction of directional cDNA libraries enriched for full-length inserts in a transcription-competent vector. Gene Anal Tech 6:33–38.

Fuchs JL (1989) [^{125}I]α-bungarotoxin binding marks primary sensory areas of developing rat neocortex. Brain Res 501:223–234.

Galzi J-L, Revah F, Bessis A, Changeux J-P (1991) Functional architecture of the nicotinic acetylcholine receptor: from electric organ to brain. Annu Rev Pharmacol 31:37–72.

Gotti C, Esparis Ogando A, Clementi F (1990) The α-bungarotoxin receptor purified from a human neuroblastoma cell line: biochemical and immunological characterization. Neuroscience 32:759–767.

Grenningloh G, Rienitz A, Schmitt B, Methfessel C, Zensen M, Beyreuther K, Gundelfinger E, Betz H (1987) The strychnine-binding subunit of the glycine receptor shows homology with nicotinic acetylcholine receptors. Nature 328:215–220.

Härfstrand A, Adem A, Fuxe K, Agnati L, Andersson K, Nordberg A (1988) Distribution of nicotinic cholinergic receptors in the rat telencephalon and diencephalon: a quantitative receptor autoradiographical study using [^{3}H]-acetylcholine, [^{125}I]-α-bungarotoxin and [^{3}H]-nicotine. Acta Physiol Scand 132:1–14.

Iino M, Ozawa S, Tsuzuki K (1990) Permeation of calcium through excitatory amino acid receptor channels in cultured rat hippocampal neurones. J Physiol (Lond) 424:151–165.

Kemp BE, Pearson RB (1990) Protein kinase recognition sequence motifs. Trends Biochem Sci 15:342–346.

Kemp G (1988) Characterization of the α-bungarotoxin binding protein from PC12 cells. In: NATO ASI series, Vol H5, Nicotinic acetylcholine receptors in the nervous system (Clementi F, ed), pp 106–117. New York: Springer.

Kemp G, Bentley L, McNamee MG, Morley BJ (1985) Purification and characterization of the α-bungarotoxin binding protein from rat brain. Brain Res 347:274–283.

Kyte J, Doolitle RF (1982) A simple method for displaying the hydropathic character of a protein. J Mol Biol 157:105–132.

Lerma J, Martin Del Rio R (1992) Chloride transport blockers prevent *N*-methyl-D-aspartate receptor-channel complex activation. Mol Pharmacol 41:217–222.

Lewis CA, Stevens C (1979) Mechanisms of ion permeation through channels in a postsynaptic membrane. In: Membrane transport processes, Vol 3 (Stevens CF, Tsien RW, eds), pp 89–103. New York: Raven.

Listerud M, Brussard AB, Devay P, Colman DR, Role LW (1991) Functional contribution of neuronal AChR subunits revealed by antisense oligonucleotides. Science 254:1518–1521.

Luetje CW, Patrick J (1991) Both α- and β-subunits contribute to the agonist sensitivity of neuronal nicotinic acetylcholine receptors. J Neurosci 11:837–845.

Mayer ML, Westbrook GL (1987) Permeation and block of *N*-methyl-D-aspartic acid receptor channels by divalent cations in mouse cultured central neurones. J Physiol (Lond) 394:501–527.

Miledi R, Parker I (1984) Chloride current induced by injection of calcium into *Xenopus* oocytes. J Physiol (Lond) 357:173–183.

Miner LL, Marks MJ, Collins AC (1986) Genetic analysis of nicotine-induced seizures and hippocampal nicotinic receptors in the mouse. J Pharmacol Exp Ther 239:853–860.

Ono JK, Salvaterra PM (1981) Snake α-toxin effects on cholinergic and noncholinergic responses of *Aplysia californica* neurons. J Neurosci 1:259–270.

Patrick J, Stallcup B (1977a) α-Bungarotoxin binding and cholinergic receptor function on a rat sympathetic nerve line. J Biol Chem 252: 8629–8633.

Patrick J, Stallcup WB (1977b) Immunological distinction between acetylcholine receptor and the α-bungarotoxin-binding component on sympathetic neurons. Proc Natl Acad Sci USA 10:4689–4692.

Paxinos G, Watson C (1986) The rat brain in stereotaxic coordinates. New York: Academic.

Revah F, Bertrand D, Gaizi J-L, Devillers-Thiery A, Mulle C, Hussy N, Bertrand S, Ballivet M, Changeux J-P (1991) Mutations in the channel domain alter desensitization of a neuronal nicotinic receptor. Nature 353:846–849.

Sands SB, Barish ME (1991) Calcium permeability of neuronal nicotinic acetylcholine receptor channels in PC12 cells. Brain Res 560: 38–42.

Schmidt J (1988) Biochemistry of nicotinic acetylcholine receptors in the vertebrate brain. Int Rev Neurobiol 30:1–38.

Schoepfer R, Conroy W, Whiting P, Gore M, Lindstrom J (1990) Brain α-bungarotoxin binding protein cDNAs and mAbs reveal subtypes of this branch of the ligand-gated ion channel gene superfamily. Neuron 5:35–48.

Seto A, Arimatsu Y, Amano T (1981) Subunit structure of α-bungarotoxin binding component in mouse brain. J Neurochem 37:210–216.

Simmons DM, Arriza JL, Swanson L (1989) A complete protocol for *in situ* hybridization of messenger RNAs in brain and other tissues with radiolabeled single-stranded RNA probes. J Histotechnol 12: 169–181.

Sine SM, Steinbach JH (1984) Agonists block currents through acetylcholine receptor channels. Biophys J 46:277–283.

Vernino S, Amador M, Luetje CW, Patrick J, Dani JA (1992) Calcium modulation and high calcium permeability of neuronal nicotinic acetylcholine receptors. Neuron 8:127–134.

Vijayaraghavan S, Pugh PC, Zhang Z, Rathouz MM, Berg DK (1992) Nicotinic receptors that bind α-bungarotoxin on neurons raise intracellular free Ca^{2+}. Neuron 8:353–362.

von Heijne G (1986) A new method for predicting signal sequence cleavage sites. Nucleic Acids Res 14:4683–4691.

Wada E, Wada K, Boulter J, Deneris E, Heinemann S, Patrick J, Swanson LW (1989) Distribution of alpha2, alpha3, alpha4, and beta2 neuronal nicotinic receptor subunit mRNAs in the central nervous system: a hybridization histochemical study in the rat. J Comp Neurol 284:314–335.

Wainer BH, Mesulam M-M (1990) Ascending cholinergic pathways in the rat brain. In: Brain cholinergic systems (Steriade M, Biesold D, eds), pp 65–119. New York: Oxford UP.

White MM, Aylwin M (1990) Niflumic and fluflenamic acids are potent reversible blockers of Ca^{2+}-activated Cl^- channels in *Xenopus* oocytes. Mol Pharmacol 37:720–724.

Wonnacott S (1986) α-Bungarotoxin binds to low-affinity nicotine binding sites in rat brain. J Neurochem 47:1706–1712.